



Bacterial cellulose/poly vinyl alcohol based wound dressings with sustained antibiotic delivery

Emel Tamahkar¹

Received: 13 November 2020 / Accepted: 27 March 2021 / Published online: 7 April 2021
© Institute of Chemistry, Slovak Academy of Sciences 2021

Abstract

The current work was aimed to prepare bacterial cellulose/poly vinyl alcohol (BC/PVA) wound dressings loaded with antibiotic which were prepared via freeze-thawing. The swelling ratio of BC/PVA hydrogels was in the range of 188–240%. The water loss percentage of BC was improved with the addition of PVA. 30% of the cumulative ampicillin delivery from BC/PVA hydrogels was achieved during 120 h suggesting significant role of PVA incorporation since 50% of ampicillin was released from BC after 24 h. BC/PVA hydrogels showed great antibacterial activity against *E.coli* and *S. aureus*. The results revealed that BC/PVA hydrogels presented great potential as wound dressings with high swelling ratio, low water loss percentage and slow antibiotic release properties.

Keywords Bacterial cellulose nanofibers · Poly vinyl alcohol · Wound dressing · Antibiotic delivery

Introduction

Wound healing is a complex process that requires effective wound management. A wound dressing is applied onto wounded area to establish an effective environment for healing process. Ideal wound dressing should provide several criteria such as removing exudates, keeping wound area moist, favouring the oxygen transfer. It should demonstrate high biocompatibility and flexibility (Simões et al. 2018). Also it should prevent the bacterial infection which promotes the healing process. The antibiotic release for a prolonged time period to the wound site becomes one of the common strategies for efficient wound treatment (Tamahkar et al. 2020). Controlled local delivery maintains the specific drug concentration at the delivery area lowering toxic side effects and systemic drug amount. Thus, the wound dressings providing sustained antibiotic release offer several advantages such as ensuring the therapeutic efficiency and decreasing the need of dressing replacements (Kimna et al. 2019).

Bacterial cellulose (BC) produced by various microorganisms such as *Agrobacterium*, *Rhizobium*, *Sarcina* and *Glucanacetobacter* is comprised of the 3-D nanofibrous network

structure. BC presents unique morphological properties having high porosity with interconnected channels (Bakhshpour et al. 2017). BC is one of the widely used biopolymers due to its unique properties such as high water holding capacity, high biocompatibility, high porosity with interconnectivity and high surface area. BC has high purity without having any lignin or hemicellulose thus avoiding the purification cost. BC owing to its high amount of surface hydroxyl groups, high surface area and high mechanical strength presents great platform for many application areas in the biomedical field (Ullah et al. 2016). BC has been utilized as wound dressing due to the combination of its superior features such as high flexibility, high water retention capacity, permeability for gas transfer, high mechanical strength and high biocompatibility. Recently, BC has attracted significant attention serving as a wound dressing with release of various drugs such as tetracycline, ibuprofen and diclofenac (Picheth et al. 2017; Luo et al. 2017).

The incorporation of functional biopolymers as a second phase is one of the modification methods to alter the drug diffusion kinetics from BC matrix (Sulaeva et al. 2020). Poly vinyl alcohol (PVA) is a FDA-approved, water-soluble biopolymer with high hydrophilicity, high biocompatibility, biodegradability, and good film forming properties. PVA was utilized widely as wound dressing material owing to its high water retention capacity, high transparency (Abdoli et al. 2020). Physically cross-linked hydrogels prepared via

✉ Emel Tamahkar
emel.irmak@btu.edu.tr

¹ Department of Bioengineering, Bursa Technical University, Bursa, Turkey

freeze-thawing have gained much interest due to the absence of consumption of toxic cross-linking agents during synthesis. In the freeze-thawing process, ice crystals develop in the amorphous region of PVA during freezing step. They induce PVA chains to fabricate concentrated domains, namely crystallites which serve as physical cross-links. During the thawing step, the ice crystals serve as porogen and PVA chains form hydrogen bonds to fabricate freeze-thawed hydrogel (Hassan and Peppas 2000; Tamahkar and Özkahraman 2015). In the literature there already existed several reports about the preparation, characterization and some applications of BC/PVA hydrogels (Li et al. 2015). Wang et al. prepared BC/PVA hydrogels with different mass ratios of BC as an artificial cornea via freeze-thawing. The resultant BC/PVA hydrogels showed increased mechanical and thermal properties in comparison with PVA. Also these hydrogels demonstrated high transparency (> 90%) than BC (Wang et al. 2010). Leitao et al. evaluated the diffusion coefficients of poly ethylene glycol (PEG) through BC and BC/PVA hydrogels. They reported that the impregnation of PVA as a second phase resulted in composite hydrogels with larger pores. Also they determined that BC/PVA hydrogels showed lower diffusion coefficients of PEG in comparison with BC since denser structure would permit less molecules to pass through the matrix (Leitão et al. 2013). Gea et al. revealed BC/PVA hydrogels displayed enhanced transparency after the incorporation of PVA into the BC structure (Gea et al. 2010).

In this study, BC/PVA wound dressings were developed as the interpenetrating network structure via physical cross-linking where PVA matrix established inside the pores of BC matrix. The BC/PVA hydrogels were characterized by FTIR-ATR and SEM measurements. The swelling ratio and water loss % of the prepared BC/PVA hydrogels were evaluated. After the antibiotic loading, drug release profiles of the hydrogels were also investigated and the release mechanism was explained with kinetic modelling. To our knowledge, this is the first study to develop BC/PVA wound dressing with ampicillin delivery.

Experimental

Materials

Acetobacter xylinum (ATCC 10245) was obtained in lyophilized form from the Agricultural Research Service Culture Collection (ARS, USA). The components utilized in the production of bacterial cellulose D(-) glucose, pectone, yeast extract, K_2HPO_4 and $KHPO_4$ were supplied in the analytical purity from Merck (Darmstadt, Germany). Polyvinyl alcohol (Mw: 86,000–125,000 kDa), ampicillin

sodium salt and glutaraldehyde were purchased from Sigma-Aldrich (St. Louis, USA).

Preparation of BC/PVA hydrogels

BC was produced from *A. xylinum* (ATCC 10245) in Hestrin-Schramm medium due to the previous work (Tamahkar et al. 2010). BC/PVA hydrogels were prepared via freeze-thawing process. Firstly, BC nanofibres were immersed into PVA solution for 24 h at 80 °C. Secondly, they were placed at - 18 °C for 24 h and then they were thawed at room temperature for 1 h. The freeze-thawing process was repeated as one, three and six cycles and they were named as BCP1, BCP3 and BCP6, respectively. The BC/PVA hydrogels were named as BCP1 when the freeze thawing cycle number was one. And similarly, they were named as BCP3 and BCP6, respectively, when the thermal cycling was repeated for three times and six times, respectively.

Characterization studies

The chemical structure of BC and BC/PVA hydrogels was investigated with FTIR-ATR measurements in the range of 600–4000 cm^{-1} using Perkin Elmer Spectrum 100. The morphological characteristics of the hydrogels were determined by SEM measurements with Quanta Feg 650 scanning electron microscope. The hydrogels were dried at room temperature and then they were covered with thin layer of gold under vacuum. The swelling tests were performed at 37 °C at pH 7.4. The dried hydrogels were put into buffer solution and weighed during determined time intervals. The swelling ratio (SR) of the hydrogels was calculated with the following Eq. (1):

$$SR = \frac{m_s - m_d}{m_d} \times 100 \quad (1)$$

where m_s is the weight of the swollen hydrogel and m_d is the weight of the dried hydrogel. In order to investigate the water loss percentage of the hydrogels, first they were swollen in water and then left under ambient temperature. The wet hydrogels were weighed at specific time intervals and the water loss percentage was calculated as follows (2):

$$\text{Water loss \%} = \frac{m_i - m_t}{m} \times 100 \quad (2)$$

where m_i is the initial weight of the wet hydrogel, m_t is the weight of the wet hydrogel at time t and m is the water content of the hydrogel. All the experiments were performed in triplicate.

In-vitro drug loading experiments

The ampicillin molecules were loaded to BC/PVA hydrogels batch-wise. The dry BC/PVA hydrogels were placed into 5 mL of ampicillin solution (5 mg/mL) at room temperature for 24 h under magnetic stirring (100 rpm). The amount of bound drug was analysed with UV–Vis spectrophotometer and calculated gravimetrically by subtracting the amount of drug of the initial solution and the amount of drug of the supernatant after the loading process. The experiments were performed in triplicate.

In-vitro drug release tests

To investigate the drug release profile of BC/PVA hydrogels, the ampicillin-loaded hydrogels were immersed into 5 mL of phosphate buffer solution (pH 7.4) at 37 °C with shaking at 50 rpm. At specific time intervals, 0.5 mL was removed from the release medium and same amount of fresh buffer solution was added into the release medium. The cumulative drug release (%) was analysed spectrophotometrically and determined with the following Eq. (3):

$$\text{Cumulative release\%} = \frac{Q_t}{Q_c} \times 100 \quad (3)$$

where Q_t is the amount of released drug at time t , and Q_c is the amount of loaded total drug of the hydrogel. The experiments were performed in triplicate.

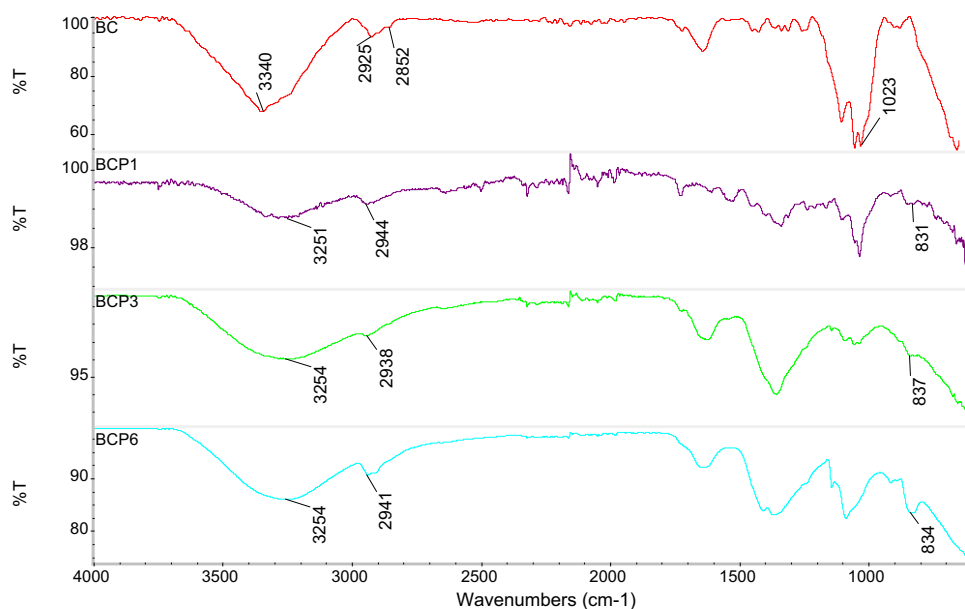
Antibacterial activity test

Antibacterial performances of BC/PVA hydrogels were evaluated by agar disc-diffusion method using *E. coli* (ATCC 25922) and *S. aureus* (ATCC 25923) that is a gram-negative and gram-positive bacterium, respectively. Prior to the tests, the bacterial strains were inoculated in the Luria Bertani (LB) growth medium (100 mL) at 37 °C for 18 h. Then, the stock cultures of *E. coli* and *S. aureus* were prepared by incubating one colony forming unit (CFU) of the bacteria in 10 mL of growth medium by adjusting to 0.5 McFarland to get a density of 1.5×10^8 CFU/mL. Lastly, the drug-loaded BC/PVA hydrogels, BC as negative control and ampicillin disc as positive control (10 µg/disc) were put onto the LB agar medium seeded with 100 µL of the bacterial suspension culture that was incubated at 37 °C for 18 h (Özkahraman et al. 2020). The antibacterial activity for BC/PVA hydrogels was determined by measuring inhibition diameters.

Results and discussion

FTIR-ATR spectrum of BC and BC/PVA hydrogels are shown in Fig. 1. The peak at 3340 cm^{-1} corresponding to –OH stretching of BC becomes broader and shifted to 3254 cm^{-1} due to the presence of intermolecular hydrogen bonding between BC and PVA. The weak band at around 2940 cm^{-1} is common for all the hydrogels representing –CH stretching. The characteristic band appeared at 1023 cm^{-1} is attributed to –C–O stretching of aliphatic alcohols of BC. The intensity of this peak was decreased for BC/PVA hydrogels owing to the interaction between the two polymeric chains. Also the band at around 834 cm^{-1}

Fig. 1 FTIR spectra of BC and BC/PVA hydrogels



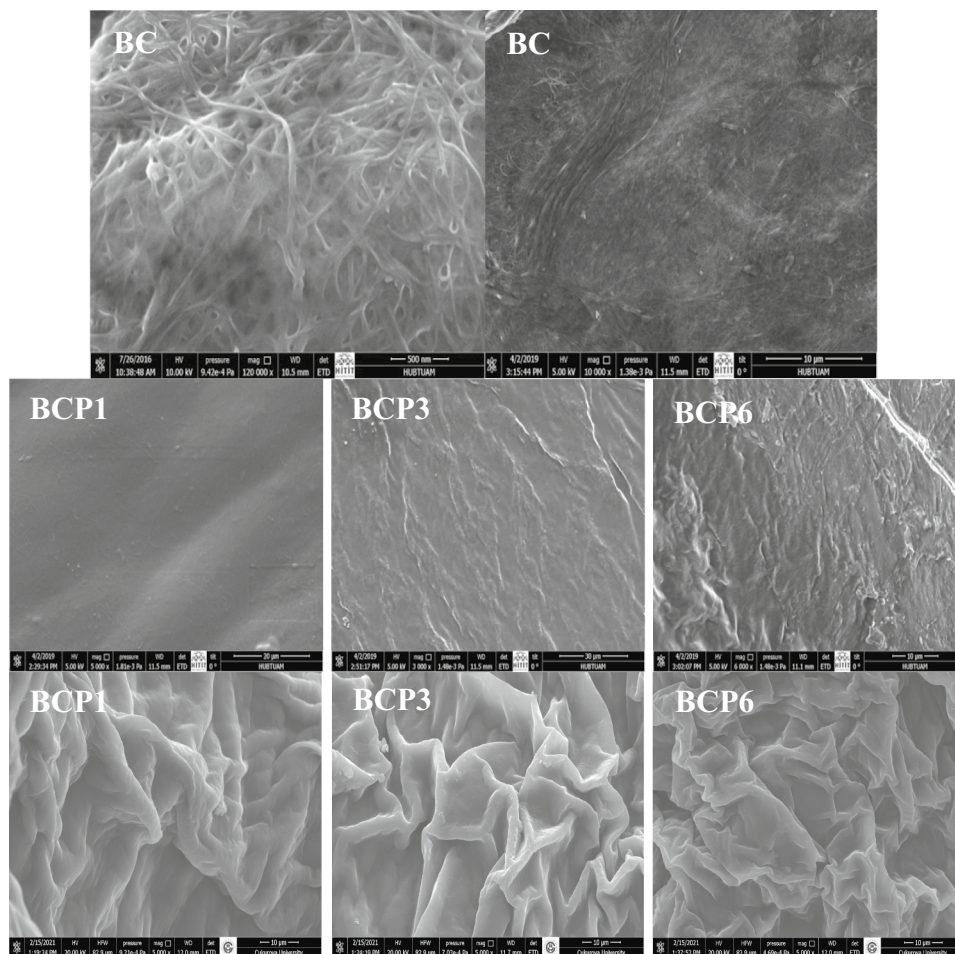
that is assigned to $-\text{CH}_2$ vibrational deformation of PVA was observed for BC/PVA hydrogels which becomes more distinct with the increase in freeze-thawing cycles due to the addition of more PVA into the BC matrix. The band at 2852 cm^{-1} that was stretching vibrational modes of $-\text{CH}$ of BC was disappeared at BC/PVA hydrogels (Stoica-Guzun et al. 2013; Asgher et al. 2017).

The morphological properties of BC/PVA hydrogels were investigated with the SEM measurements (Fig. 2). The 3-D network structure of BC hydrogels was observed. The incorporation of PVA throughout the BC network was clearly determined from the SEM images due to the denser structure of BC/PVA hydrogels. BC/PVA hydrogels were fabricated as the interpenetrating network via physical cross-linking with freeze-thawing cycles. The integration of PVA matrix with BC was occurred with two steps: at first PVA filled the pores of the BC and then PVA network was constructed throughout the BC nanofibrous matrix during the thermal cycling resulting in an interpenetrating network structure (Qiu and Netravali 2012). It was clearly determined from the SEM photographs that porosity of the hydrogels was increased with increased number of freeze-thawing cycles.

Also it was observed that the thickness of the prepared BC/PVA hydrogels was increased with increased amount of PVA. The thickness of the plain BC hydrogels was measured as $0.15\text{ }\mu\text{m}$, while BC/PVA hydrogels for BCP1, BCP3 and BCP6 were found as 0.2 , 0.4 and $0.5\text{ }\mu\text{m}$, respectively. From SEM photographs, two diameters were taken corresponding to longitudinal axis of the pore (D1) and transversal axis of the pore (D2) using ImageJ software (<http://rsb.info.nih.gov/ij/>) by measuring at least 30 pores per each image. D1 was determined in the range of $12\text{--}16\text{ }\mu\text{m}$ and D2 was measured as $4\text{--}8\text{ }\mu\text{m}$. These results indicated the success of the preparation method of BC/PVA hydrogels.

The swelling is one of the important properties for drug delivery applications. The swelling of hydrogels occurs in three steps as; (1) initially, hydrogel swells fast owing to the surface hydrophilicity, (2) then, diffusion of water molecules through the hydrogel matrix slows down, (3) lastly, water uptake reaches an equilibrium. The swelling capacity of BC and BC/PVA hydrogels were plotted against time (Fig. 3). The water absorption amount increased gradually with time until it reached an equilibrium value. The time required to reach the swelling equilibrium of BC and BC/

Fig. 2 SEM images of BC and BC/PVA hydrogels



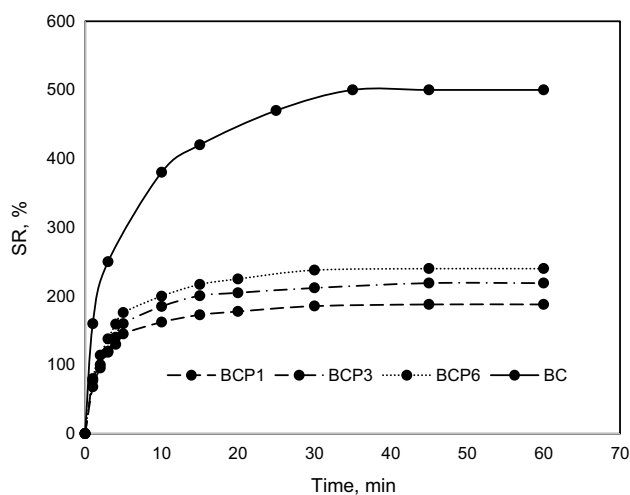


Fig. 3 Swelling ratio (%) of BC and BC/PVA hydrogels

PVA hydrogels was found as 30 min and 45 min, respectively. The macroporous structure of the prepared BC/PVA hydrogels resulted in the fast transport of water molecules through the polymeric matrix (Daza Agudelo et al. 2018). The swelling percentages of BCP1, BCP3 and BCP6 hydrogels were 188, 219 and 240%, respectively, since the swelling percentage of BC was 500%. The high hydrophilic nature of the BC and BC/PVA hydrogels provided high swelling capacity. The swelling amount was decreased with the incorporation of PVA network into BC. This may be caused by the formation of second polymeric network in the pores of BC matrix via physical cross-linking reducing the permeability of water molecules (Dobre and Stoica-Guzun 2013). The swelling ratio of BC/PVA hydrogels increased with the increased number of freeze-thawing cycles since gelation amount increases with physical cross-linking via thermal cycling.

The ratio of water loss of the BC/PVA hydrogels was presented in Fig. 4. The water release rate of BC was the largest among the hydrogels. The dehydration was reduced due to the formation of interpenetrating network with PVA. The amount of water loss decreased with increasing the number of freeze-thawing cycles. The results suggest that the dehydration properties were enhanced with the incorporation of PVA into BC matrix and with the freeze-thawing cycles for BC/PVA hydrogels. This may be caused by the smaller pores of BC/PVA hydrogels after the fabrication of interpenetrating network structure throughout the BC matrix. The water retention capability of the hydrogels is an significant issue for the applications of wound dressing or artificial skin (Luo et al. 2016). The management of water loss from wound is one of the important issues for wound treatment since dehydration causes reduction in body temperature which increases the metabolic rate resulting in

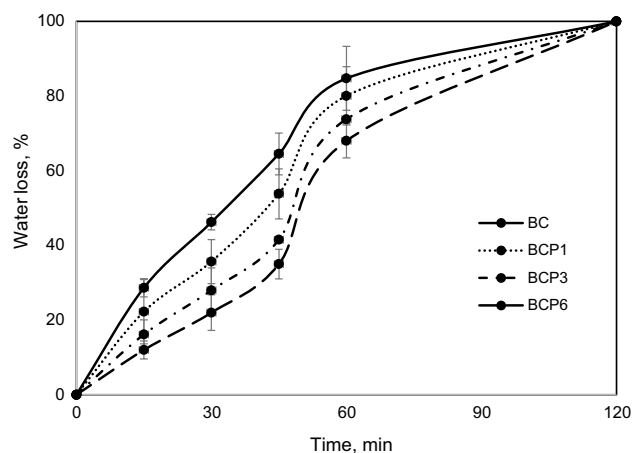


Fig. 4 The percentage of water loss of BC and BC/PVA hydrogels

delay of the healing process. The wound dressing should provide an adequate moist in the wound site (Khorasani et al. 2018). BC/PVA hydrogels exhibit their great potential since they can facilitate wound healing with good swelling and deswelling properties.

To gain information about mechanisms of swelling and de-swelling, power law was used to calculate the kinetic parameters of swelling (4) and de-swelling of BC and BC/PVA hydrogels (5) noting that these equations are valid for the initial 60% of the total experimental data:

$$\frac{M_t}{M_e} = k_s t^{n,s} \quad (4)$$

$$\frac{W_t}{W_e} = k_d t^{n,d} \quad (5)$$

Here, M_t and M_e are the swelling ratio of hydrogels at time t and swelling ratio at equilibrium, respectively. W_t and W_e are the de-swelling ratio at t and at equilibrium, respectively. Fick constants of swelling and de-swelling are k_s and k_d , respectively. The swelling constant is n,s and the de-swelling constant is n,d . The kinetic parameters of swelling and de-swelling and the regression coefficients (R^2) were summarized in Table 1. The value of n is ≤ 0.5 when the process is based on Fickian law since it fits to non-Fickian model if n is between 0.5 and 1. All the experimental data fitted well with the power law due to high correlation coefficients.

It can be stated that the mechanism of swelling of BC follows non-Fickian diffusion suggesting the transport mechanism is both diffusion-controlled and chain relaxation-controlled. However the swelling process of all BC/PVA hydrogels follows Fickian diffusion due to n values indicating the swelling was diffusion-controlled since the relaxation rate of polymer chains is higher than the diffusion rate

Table 1 Kinetic parameters of swelling and de-swelling

	Swelling			De-swelling		
	n_s	k_s	R^2	n_d	k_d	R^2
BC	0.52	0.36	0.95	0.49	0.085	0.96
BCP1	0.30	0.41	0.93	0.50	0.077	0.99
BCP3	0.37	0.36	0.97	0.54	0.069	0.97
BCP6	0.39	0.35	0.94	0.69	0.024	0.99

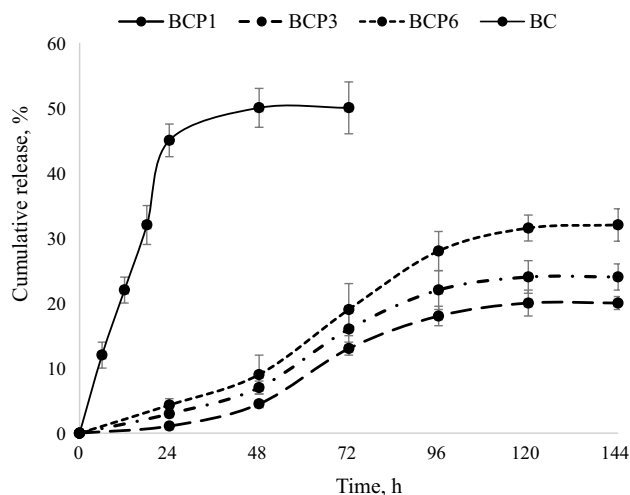
Table 2 Loading amounts of ampicillin onto BC and BC/PVA hydrogels

	Loading amount of Amp, mg/g
BC	122 ± 9.8
BCP1	54.8 ± 5.4
BCP3	42.8 ± 4.7
BCP6	38.5 ± 4.3

of the solvent through the polymeric matrix. The dominant mechanism of de-swelling of BC and BC/PVA hydrogels was determined to be Fickian and non-Fickian, respectively (Karimi and Wan Daud 2016).

The amount of ampicillin loading was analysed using UV–Vis spectroscopy and loading amount of ampicillin to BC and BC/PVA hydrogels were shown in Table 2. The ampicillin loading capacity of BC hydrogel was 122 mg/g; however, the loading content of BC/PVA hydrogels was decreased from 54.8 to 38.5 mg/g with the increase of freeze-thawing cycles of the fabrication process from 1 to 6. The accessible binding sites of ampicillin onto the BC hydrogel were reduced with the integration of the second polymeric network. Due to the increased number of freeze-thawing cycles, denser polymeric structure was constructed with the increased physical cross-linking (Figuroa-Pizano et al. 2018). However, the number of available sites for ampicillin was decreased. The hydroxyl groups of BC and PVA enable the adsorption of ampicillin molecules onto the prepared hydrogels via hydrogen bonding.

Figure 5 illustrated the cumulative release profile of ampicillin from BC and BC/PVA hydrogels at pH 7.4 at 37 °C. Almost all of the bound ampicillin onto BC was released after 24 h. The ampicillin release from BC/PVA hydrogels reached an equilibrium after 120 h indicating a long-term antibiotic release. The controlled release of ampicillin from BC/PVA based hydrogels with respect to plain BC can be inferred to the formation of denser structure with the impregnation of PVA as a second network throughout the BC matrix leading the hindrance for drug diffusion. The release of chloramphenicol from biodegradable BC hydrogels was reported as 99% after 24 h (Laçin 2014). The slow release of antibiotics from wound dressings is crucial to prevent bacterial infections during the treatment period. The results offer that BC/PVA hydrogels

**Fig. 5** Drug release profiles of BC and BC/PVA hydrogels

demonstrate the applicability as wound dressings delivering antibiotics for 120 h.

The mathematical modelling of the release kinetics was performed using zero-order, first-order, Higuchi and Korsmeyer-Peppas kinetic models to clarify release behaviour and transport mechanism (Özkahraman and Tamahkar 2017). Zero-order model is independent of drug concentration however, drug release of first-order kinetic model is dependent on concentration. Higuchi model defines drug release regarding to diffusion based on Fick's law (Bal et al. 2016). Korsmeyer-Peppas model describes drug release as diffusion of drug and erosion of polymer matrix and determines the transport mechanism of release with respect to diffusional constant, n as follows: if $n \leq 0.5$, release fits to Fickian diffusion; if $0.5 < n < 1$, release corresponds to non-Fickian diffusion model; if $n = 1$, release follows Case II transport; if $n > 1$, then transport mechanism is super case II (Peppas and Sahlin 1989).

$$Q_t = Q_0 + k_0 t \quad (6)$$

$$\ln Q_t = \ln Q_0 - k_1 t \quad (7)$$

$$Q_t = k_H \sqrt{t} \quad (8)$$

Table 3 Release kinetic parameters of BC and BC/PVA hydrogels

	BC	BCP1	BCP3	BCP6
Zero-order				
k_0	0.65	0.17	0.19	0.25
R^2	0.72	0.93	0.88	0.93
First-order				
k_1	0.58	0.023	0.018	0.017
R^2	0.87	0.79	0.81	0.86
Higuchi				
k_H	8.85	3.11	3.37	4.41
R^2	0.90	0.96	0.92	0.96
Korsmeyer-Peppas				
n	0.72	1.72	1.29	1.21
$k_K \times 10^{-3}$	73.15	0.26	2.03	2.93
R^2	0.93	0.95	0.93	0.97

$$\frac{Q_t}{Q_{eq}} = k_K t^n \quad (9)$$

where Q_t is the release amount of drug at time t , Q_0 is the initial amount of drug, Q_{eq} is the amount of drug release at equilibrium, k_0 , k_1 , k_H and k_K are release constants of zero-order, first-order, Higuchi and Korsmeyer-Peppas models, respectively, and n is the diffusion exponent.

Due to regression coefficients listed in Table 3, the drug release from BC/PVA hydrogels was determined to follow Higuchi and Korsmeyer-Peppas models. The mechanism of ampicillin release from BC/PVA hydrogels fitted well to super case II transport due to $n > 1$ which refers to the erosion of the polymeric materials (Tamahkar et al. 2019).

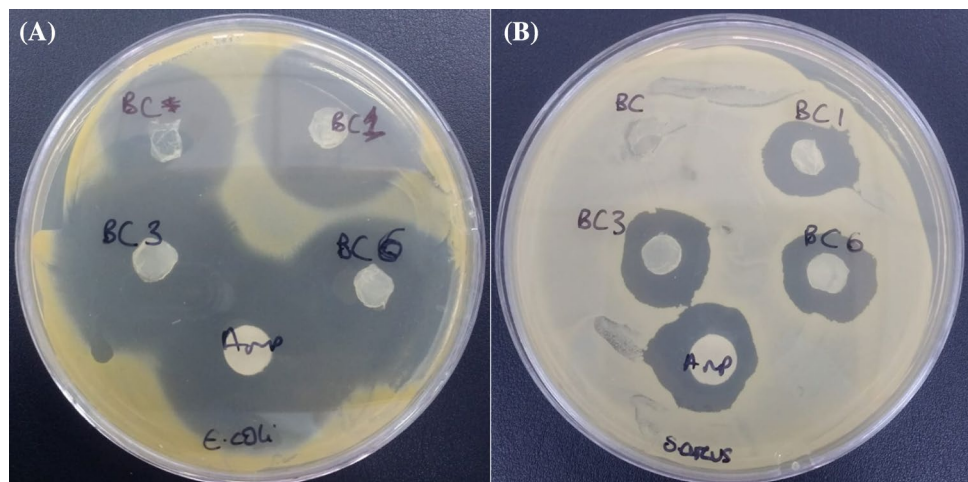
Antibacterial activity of BC/PVA hydrogels was examined with *E. coli* and *S. aureus* by agar disc diffusion (Fig. 6). The antibacterial activity of BC, BCP1, BCP3, BCP6 hydrogels with respect to the inhibition zone diameters was measured against *E. coli* as 26, 33, 35 and 38 mm, respectively,

while inhibition zone of ampicillin disc was found as 36 mm. The inhibition zone diameters of BC, BCP1, BCP3, BCP6 hydrogels were as 0, 17, 18 and 19 mm against *S. aureus* since ampicillin disc showed inhibition zone as 21 mm. The ampicillin-loaded BC/PVA hydrogels all demonstrated great antibacterial activity against *E. coli* and good antibacterial activity against *S. aureus* implying them as alternative wound dressings with antibiotic release (Ye et al. 2019).

Conclusions

BC has attracted tremendous interest both as a wound dressing and a drug delivery vehicle due to its hydrophilicity, biocompatibility, flexibility and interconnected nanofibrous structure. The impregnation of PVA into BC structure enhances some features to improve the performance for wound treatment. The characteristics of BC/PVA hydrogels as a biomaterial were evaluated previously by several research groups. Herein, the potential of BC/PVA hydrogels was aimed to investigate as a wound dressing with prolonged antibiotic release. The BC/PVA hydrogels were prepared via freeze-thawing with different thermal cycles of one, three and six. PVA matrix was formed throughout the pores of BC network structure producing an interpenetrating network. The properties of percentage of water loss and cumulative drug release of BC were improved with the addition of PVA as well as with the increased number of thermal cycles.

Fig. 6 The photograph of antibacterial activity assay of BC, BC/PVA hydrogels and ampicillin disc against **a** *E. coli*, **b** *S. Aureus*



Acknowledgements The financial support from the Scientific Projects Coordination Unit of Hitit University under the project number MUH19002.16.001 is gratefully acknowledged. The author is grateful for the laboratory support of Balikesir University, Science and Technology Research and Application Center (BUSTRAC) and Department of Food Engineering, Cargill Inc. The author is also thankful to Dr. Işık Perçin and Gülsen Bayrak for the laboratory support for antibacterial activity tests.

Declaration

Conflict of interest There is no conflict of interest.

References

- Abdoli M, Sadrjavadi K, Arkan E, Zangeneh MM, Moradi S, Zangeneh A, Mohsen S, Khaledian S (2020) Polyvinyl alcohol/gum tragacanth/graphene oxide composite nanofiber for antibiotic delivery. *J Drug Deliv Sci Technol*. <https://doi.org/10.1016/j.jddst.2020.102044>
- Asgher M, Ahmad Z, Iqbal HMN (2017) Bacterial cellulose-assisted de-lignified wheat straw-pva based bio-composites with novel characteristics. *Carbohydr Polym* 161:244–252. <https://doi.org/10.1016/j.carbpol.2017.01.032>
- Bakhshpour M, Tamahkar E, Andaç M, Denizli A (2017) Affinity binding of proteins to the modified bacterial cellulose nanofibers. *J Chromatogr B* 1052:121–127. <https://doi.org/10.1016/j.jchromb.2017.03.021>
- Bal A, Özkahraman B, Özbaş Z (2016) Preparation and characterization of ph responsive poly(methacrylic acid-acrylamide-n-hydroxyethyl acrylamide) hydrogels for drug delivery systems. *J Appl Polym Sci*. <https://doi.org/10.1002/app.43226>
- Daza Agudelo JI, Badano JM, Rintoul I (2018) Kinetics and thermodynamics of swelling and dissolution of pva gels obtained by freeze-thaw technique. *Mater Chem Phys* 216:14–21. <https://doi.org/10.1016/j.matchemphys.2018.05.038>
- Dobre ML, Stoica-Guzun A (2013) Antimicrobial ag-polyvinyl alcohol-bacterial cellulose composite films. *J Biobased Mater Bioenergy* 7:157–162
- Figueroa-Pizano MD, Vélaz I, Peñas FJ, Zavala-Rivera P, Rosas-Durazo AJ, Maldonado-Arce AD, Martínez-Barbosa ME (2018) Effect of freeze-thawing conditions for preparation of chitosan-poly (vinyl alcohol) hydrogels and drug release studies. *Carbohydr Polym* 195:476–485. <https://doi.org/10.1016/j.carbpol.2018.05.004>
- Gea S, Bilotti E, Reynolds CT, Soykeabkeaw N, Peijs T (2010) Bacterial cellulose–poly(vinyl alcohol) nanocomposites prepared by an in-situ process. *Mater Lett* 64:901–904. <https://doi.org/10.1016/j.matlet.2010.01.042>
- Hassan CM, Peppas NA (2000) Biopolymers PVA hydrogels, anionic polymerisation nanocomposites. Springer, Berlin
- Karimi A, Wan Daud WMA (2016) Comparison the properties of pva/na+-mmt nanocomposite hydrogels prepared by physical and physicochemical crosslinking. *Polym Compos* 37:897–906. <https://doi.org/10.1002/pc.23248>
- Khorasani MT, Joorabloo A, Moghaddam A, Shamsi H, Mansoori-Moghadam Z (2018) Incorporation of zno nanoparticles into heparinised polyvinyl alcohol/chitosan hydrogels for wound dressing application. *Int J Biol Macromol* 114:1203–1215. <https://doi.org/10.1016/j.ijbiomac.2018.04.010>
- Kimna C, Tamburaci S, Tihminlioglu F (2019) Novel zein-based multilayer wound dressing membranes with controlled release of gentamicin. *J Biomed Mater Res B Appl Biomater* 107:2057–2070. <https://doi.org/10.1002/jbm.b.34298>
- Laçın NT (2014) Development of biodegradable antibacterial cellulose based hydrogel membranes for wound healing. *Int J Biol Macromol* 67:22–27. <https://doi.org/10.1016/j.ijbiomac.2014.03.003>
- Leitão AF, Silva JP, Dourado F, Gama M (2013) Production and characterization of a new bacterial cellulose/poly(vinyl alcohol) nanocomposite. *Materials*. <https://doi.org/10.3390/ma6051956>
- Li L, Ren L, Wang L, Liu S, Zhang Y, Tang L, Wang Y (2015) Effect of water state and polymer chain motion on the mechanical properties of a bacterial cellulose and polyvinyl alcohol (bc/pva) hydrogel. *RSC Adv* 5:25525–25531. <https://doi.org/10.1039/C4RA11594E>
- Luo X, Zhang H, Cao Z, Cai N, Xue Y, Yu F (2016) A simple route to develop transparent doxorubicin-loaded nanodiamonds/cellulose nanocomposite membranes as potential wound dressings. *Carbohydr Polym* 143:231–238. <https://doi.org/10.1016/j.carbpol.2016.01.076>
- Luo H, Ao H, Li G, Li W, Xiong G, Zhu Y, Wan Y (2017) Bacterial cellulose/graphene oxide nanocomposite as a novel drug delivery system. *Curr Appl Phys* 17:249–254. <https://doi.org/10.1016/j.cap.2016.12.001>
- Özkahraman B, Tamahkar E (2017) Carbon nanotube based polyvinylalcohol-polyvinylpyrrolidone nanocomposite hydrogels for controlled drug delivery applications. *Anadolu Univ J Sci Technol A Appl Sci Eng* 18:543–553. <https://doi.org/10.18038/aubtda.322138>
- Özkahraman B, Tamahkar E, İdil N, KılıçSuloglu A, Perçin I (2020) Evaluation of hyaluronic acid nanoparticle embedded chitosan-gelatin hydrogels for antibiotic release. *Drug Dev Res*. <https://doi.org/10.1002/ddr.21747>
- Peppas NA, Sahlin JJ (1989) A simple equation for the description of solute release. Iii. Coupling of diffusion and relaxation. *Int J Pharm* 57:169–172
- Picheth GF, Pirich CL, Sierakowski MR, Woehl MA, Sakakibara CN, de Souza CF, Martin AA, da Silva R, de Freitas RA (2017) Bacterial cellulose in biomedical applications: a review. *Int J Biol Macromol* 104:97–106. <https://doi.org/10.1016/j.ijbiomac.2017.05.171>
- Qiu K, Netravali AN (2012) Bacterial cellulose-based membrane-like biodegradable composites using cross-linked and noncross-linked polyvinyl alcohol. *J Mater Sci* 47:6066–6075. <https://doi.org/10.1007/s10853-012-6517-9>
- Simões D, Miguel SP, Ribeiro MP, Coutinho P, Mendonça AG, Correia IJ (2018) Recent advances on antimicrobial wound dressing: a review. *Eur J Pharm Biopharm* 127:130–141. <https://doi.org/10.1016/j.ejpb.2018.02.022>
- Stoica-Guzun A, Stroescu M, Jipa I, Dobre L, Zaharescu T (2013) Effect of γ irradiation on poly(vinyl alcohol) and bacterial cellulose composites used as packaging materials. *Radiat Phys Chem* 84:200–204. <https://doi.org/10.1016/j.radphyschem.2012.06.017>
- Sulaeva I, Hettegger H, Bergen A, Rohrer C, Kostic M, Konnerth J, Rosenau T, Potthast A (2020) Fabrication of bacterial cellulose-based wound dressings with improved performance by impregnation with alginate. *Mater Sci Eng C* 110:110619. <https://doi.org/10.1016/j.msec.2019.110619>
- Tamahkar E, Özkahraman B (2015) Potential evaluation of pva-based hydrogels for biomedical applications. *Hittite J Sci Eng* 2:165–171. <https://doi.org/10.17350/HJSE19030000021>
- Tamahkar E, Babaç C, Kutsal T, Pişkin E, Denizli A (2010) Bacterial cellulose nanofibers for albumin depletion from human serum. *Process Biochem* 45:1713–1719. <https://doi.org/10.1016/j.procbio.2010.07.007>

- Tamahkar E, Bakhshpour M, Denizli A (2019) Molecularly imprinted composite bacterial cellulose nanofibers for antibiotic release. *J Biomater Sci Polym Ed* 30:450–461. <https://doi.org/10.1080/09205063.2019.1580665>
- Tamahkar E, Özkahraman B, Süloğlu AK, İdil N, Perçin I (2020) A novel multilayer hydrogel wound dressing for antibiotic release. *J Drug Deliv Sci Technol* 58:101536. <https://doi.org/10.1016/j.jddst.2020.101536>
- Ullah H, Santos HA, Khan T (2016) Applications of bacterial cellulose in food, cosmetics and drug delivery. *Cellulose* 23:2291–2314. <https://doi.org/10.1007/s10570-016-0986-y>
- Wang J, Gao C, Zhang Y, Wan Y (2010) Preparation and in vitro characterization of bc/pva hydrogel composite for its potential use as artificial cornea biomaterial. *Mater Sci Eng C* 30:214–218. <https://doi.org/10.1016/j.msec.2009.10.006>
- Ye S, Jiang L, Su C, Zhu Z, Wen Y, Shao W (2019) Development of gelatin/bacterial cellulose composite sponges as potential natural wound dressings. *Int J Biol Macromol* 133:148–155

Publisher's Note Springer Nature remains neutral with regard to jurisdictional claims in published maps and institutional affiliations.